Geophysical Research Letters

RESEARCH LETTER
10.1029/2020GL088762

Key Points:
- Gamma functions represent ice particle size distributions significantly better than exponential functions
- Intercept, slope, and shape parameters in fitted gamma functions for ice particle size distributions are mutually dependent
- Wind speeds play an important role in controlling ice particle size distributions, especially for snow particles

Correspondence to:
H. Leighton,
hua.leighton@noaa.gov

Citation:
Leighton, H., Black, R., Zhang, X., Marks, F. D. Jr, & Gopalakrishnan, S. G. (2020). Ice particle size distributions from composites of microphysics observations collected in tropical cyclones. *Geophysical Research Letters*, *47*, e2020GL088762. https://doi.org/10.1029/2020GL088762

Received 6 MAY 2020
Accepted 17 JUL 2020
Accepted article online 29 JUL 2020

Ice Particle Size Distributions From Composites of Microphysics Observations Collected in Tropical Cyclones

Hua Leighton[1,2], Robert Black[2], Xuejin Zhang[2], Frank D. Marks Jr[2], and Sundararaman G. Gopalakrishnan[2]

[1]Rosenstiel School of Marine and Atmospheric Science, University of Miami, Miami, FL, USA, [2]NOAA/AOML/Hurricane Research Division, Miami, FL, USA

Abstract Ice microphysics observations collected from eight flights into tropical cyclones (TCs) were analyzed to examine the performance of exponential versus gamma functions in representing the particle size distributions (PSDs) for cloud ice, snow, and graupel. Eighty-four percent (87%) of cloud ice (snow) PSDs are above the correlation threshold of 0.9 between observations and the corresponding fitted curves by gamma fits, while only 43% (55%) of cloud ice (snow) PSDs by exponential fits. Sixteen percent of graupel PSDs are above the threshold by gamma fits but none by exponential fits. The intercept, slope, and shape in gamma functions are mutually dependent. When one among the three parameters is prescribed, the other two can be empirically rendered from the mutual-dependence relationship. Counterintuitively, temperature does not play a conspicuous role in controlling ice PSDs in the TC environment but horizontal winds do, especially for snow, through the breakup process.

Plain Language Summary A crucial component of numerical weather forecasts is to realistically represent how liquid and solid water particles form, grow, and dissipate. Accurate distributions of the sizes of these particles are needed. We analyzed observations of solid water particles from eight research flights into tropical cyclones to estimate these distributions in this study. Our results showed that gamma functions can represent these distributions more realistically than exponential functions. The intercept, slope, and shape in gamma functions are mutually dependent. This mutual dependence simplifies the application of the gamma functions to microphysical process modeling. Our results also showed for the first time that ice particle size distributions do not depend on temperature in the tropical cyclone environment. Instead, horizontal wind speeds play an important role in controlling the ice particle size distributions, especially for snow.

1. Introduction

Microphysical processes play a significant role in the distribution of diabatic heating, which is one of the primary driving forces of a TC's intensity change. The realistic representation of microphysical processes in numerical models is crucial to simulating the TC's intensity and evolution accurately (Willoughby et al., 1984; Lord & Lord, 1988; Lord et al., 1984; McFarquhar & Black, 2004).

Due to the computational resource limitations, most numerical weather prediction models use bulk microphysical parameterization schemes to represent the collective effects of microphysical processes governing hydrometeor particle formation, growth, and dissipation. Various assumptions, such as particle size distribution (PSD), mass-diameter-terminal velocity relationship, and physical processes contributing to the sources and sinks of each hydrometeor category, are made in the bulk microphysics parameterization scheme. Yet the assumptions in current microphysics schemes (e.g., Hong & Lim, 2006; Lin et al., 1983; Thompson et al., 2008) are based on observations obtained in non-TC environments, and hence their suitability for use in simulations of TCs is unknown.

A few studies so far have used microphysics observations collected in TC environments to explore the microphysics assumptions. Heymsfield et al. (2006) indicated that the slope of the fitted exponential PSD was distinctly different close to the eye than outside of that region by using ice microphysics observations collected at altitudes from 8.5 to 11.9 km in Hurricane Humberto (2001). McFarquhar and Black (2004) showed the

significant impact on the mass-weighted fall speed associated with the fitted exponential PSD using the ice microphysics observations collected in Hurricanes Norbert (1984) and Hurricane Emily (1987).

Both studies did not evaluate the performance of the exponential function assumption of the fitted ice PSD. Moreover, the limited sample size may hamper the application of their findings to microphysics parameterization schemes.

Since the 1970s TC field campaigns by NOAA and NASA have collected in situ rain and ice data for microphysical process research. Previous studies suggested that ice microphysics is not only fundamentally important but also imposes the biggest uncertainty in its representations in microphysics schemes due to its large degree of complexity (e.g., Shapiro et al., 1988; Willoughby et al., 1984). Understanding of ice hydrometeor distributions in TCs was improved by using these data obtained from TC field experiments (e.g., Black, 1990; Black et al., 1994; Black & Hallett, 1986, 1999; Houze et al., 1992). However, these results are yet to be translated into improving microphysics parameterization schemes in TC modeling. Among all the assumptions made in the microphysics scheme, the assumption of the PSD function is critical since most of the parameterized processes in the microphysics schemes, such as accretion, melting, evaporation, or deposition, involve at least one parameter from the functions that represent the PSDs.

In this study, we use the available ice microphysics observations to compare the exponential and gamma fits for three solid hydrometeor categories: cloud ice, snow, and graupel, examine the mutual dependence of parameters in the fitting functions, and explore the relationship between parameters in the fitted functions and environmental variables. The remainder of the paper is organized as follows. In section 2 the data description is discussed; in section 3 the performance of exponential and gamma fits for solid hydrometeor categories are compared; in section 4 the mutual dependence of parameters in gamma fits are examined; in section 5 the relationships between the parameters in gamma fits and environmental variables are explored. A discussion and conclusion are given in section 6.

2. Data Description

The ice microphysics observation used in this study were from eight flights: one flight from Hurricane Irene (1981), three flights from Hurricane Norbert (1984), one flight from Hurricane Newton (1986), one flight from Hurricane Emily (1987), one flight from Hurricane Claudette (1991), and one flight from Hurricane Tina (1992). There are over 10,000 microphysics observations which were sampled in the TC eyewall where deep convection took place and the stratiform region outside of the eyewall at or above the melting level. The temperature ranges from −10°C to 0°C. These data were collected through two-dimensional cloud (2DC) and precipitation (2DP) probes that were installed on the NOAA P-3 aircrafts. Black and Hallett (1986) and Black (1990) described the data collection and analysis procedure in details. The 2DC observations with sample volume between 1 and 4 L and 2DP observations with sample volume between 4 and 16 L within 6 s are selected for this study. Ice, graupel, and snow particles all depend on the area/perimeter ratio for identification. For example, a perfect circle has an APR of R/6, and every other particle APR is greater than that. Known ice particles "close" to this ideal are called "graupel," particles with a length greater than 6 times the width are called "cloud ice" and ice particles between these extremes are labeled "snow." There are over 8,000 samples of cloud ice, over 6,000 samples of snow, and over 3,000 samples of graupel used in this study.

In addition to ice microphysics observation, corresponding flight-level observations of environmental variables, such as temperature, humidity, and wind, were also incorporated in this study in order to study the relationship between microphysics properties and the environment variables. The observations of these environmental variables, which were taken at the same locations as the microphysics observation but at 1 s frequency, are averaged over 6 s time window corresponding to the sample time of microphysics observations.

3. The PSD Function: Exponential Versus Gamma PSD

The PSD of hydrometeors can be represented by an exponential function or gamma function (Hansen & Travis, 1974; Marshall & Palmer, 1948; Sekhon & Srivastava, 1970; Ulbrich, 1983). The number distribution function $N(D)$ for a gamma function is typically given by

$$N(D) = N_0 D^{\mu} e^{-\lambda D} \tag{1}$$

where D is the maximum dimension of the particle, N_0 is the intercept parameter, λ is the slope, and μ is the shape parameter. When μ equals zero, a gamma function reduces to an exponential function, as in Equation 2.

$$N(D) = N_0 e^{-\lambda D} \tag{2}$$

In this section, we will explore the distribution of slope (λ) and intercept ($\log_{10}N_0$) for exponential and gamma fits and compare the overall performance of exponential and gamma fits. Each observed PSD is fitted with a gamma function (Equation 1) and an exponential function (Equation 2), respectively. A least squares method, which minimizes the difference between the observed PSD and its fitted PSD, is used to find the optimal parameters for the fitted function. The correlation coefficient between the observed PSD and fitted PSD, following Heymsfield et al. (2002) and McFarquhar et al. (2006), is adopted to evaluate the performance of the fitted function. A correlation threshold of above 0.9 (Heymsfield et al., 2002; McFarquhar et al., 2006) is used as a criterion for accepting the fitted function for representing the observed PSD. Cumulative distribution functions of correlation coefficients for exponential and gamma fits are used to quantify the overall performance of exponential and gamma fits.

Figure 1a shows the scatter plot of slope (λ) versus intercept ($\log_{10}N_0$) for exponential fits of cloud ice PSDs. It can be seen that the intercept increases rapidly with the slope when the slope is <8 and the data points are characterized by relatively low correlation coefficients (<0.9). When the slope is >8, the data points are scattered and characterized by high correlation coefficients (>0.9). This suggests that a significant portion of cloud ice PSDs cannot be realistically represented by exponential fits. This is confirmed in Figure 1d, which shows only 43.2% of data points have correlation coefficient greater than 0.9.

Figure 1b is the same as Figure 1a but for snow PSDs. Similar to the distribution for cloud ice PSDs in Figure 1a, the intercept increases quickly with the slope when the slope is <3. The intercept increases much more slowly with the slope when the slope is >3. Meanwhile, the data points are much more scattered and characterized by high correlation coefficients. Figure 1e shows that 55.3% of data points have correlation coefficients greater than 0.9.

Figure 1c is the same as Figure 1a but for graupel PSDs. As it can be seen, the distribution is completely different from that for ice and snow. The correlation coefficients are very low as denoted by the color scale in Figure 1c. Figure 1f confirmed that there are no data points that have correlation coefficient greater than 0.9.

Figure 1 reveals that the performance of exponential fits for representing graupel PSDs is very poor. There is only about half of observed PSDs of cloud ice and snow and none of observed graupel PSDs that can be realistically represented by exponential fits.

Figure 2a shows the scatter plot of slope versus intercept for gamma fits of cloud ice PSDs. As pointed out by McFarquhar et al. (2015), the introduction of D^{μ} in gamma function makes it difficult to interpret the physical meaning of N_0 since the unit of N_0 is different from the number of concentration N. This leads to the values of N_0 in gamma fits that are much larger than those in exponential fits (Figure 2a). Despite the unphysical meaning of N_0, the main cluster of $\log_{10}N_0$ versus λ distribution shows a clear relationship between them. The correlation coefficients of the gamma fits with observed PSDs are very high overall. A few data points with low correlation coefficients deviate from the main cluster. Figure 2d shows that more than 84.4% of the data points have correlation coefficients greater than 0.9. This percentage almost doubles that from the exponential fits.

Figure 2b is the same as Figure 2a but for snow PSDs. As can be seen, similar to the distribution in Figure 2a, the data points are highly clustered in an almost linear manner. A few data points that significantly deviate from the main cluster are characterized by very small correlation coefficients (blue dots). Figure 2e shows that more than 87% of data points have correlation coefficients greater than 0.9. This percentage is about 60% more than that of the snow PSDs using exponential fits (Figure 1e).

Figure 2c is the same as Figure 2a but for graupel PSDs. As can be seen, all data points are organized into an almost linear relationship. The data points with smaller slope (≤10) are characterized by low values of

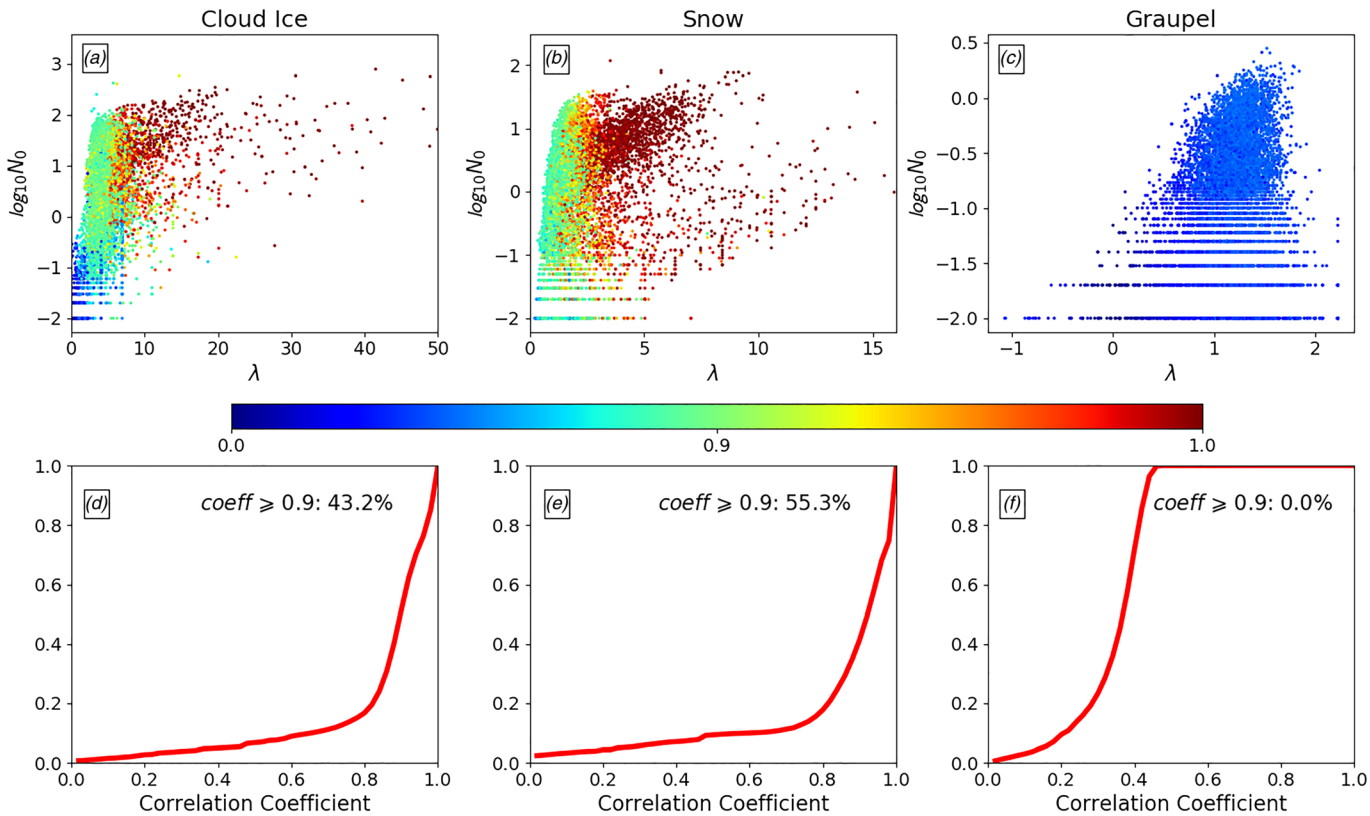

Figure 1. Scatter plot of λ versus $\log_{10}(N_0)$ of exponential fit for (a) cloud ice (b) snow, and (c) graupel. Panels (d)–(f) are the cumulative distribution function of correlation coefficient between fitted PSD (exponential form) and observed PSD for ice, snow, and graupel, respectively. The percentage with correlation coefficient greater than 0.9 is denoted in each plot.

correlation coefficients. Most of the data points with higher correlation coefficients are with slope greater than 10. Overall, the correlation coefficients for gamma fitted PSDs of graupel are much lower than that for both cloud ice and snow PSDs. One of the main reasons is that the size spectrum is often discontinuous for the observed graupel PSD. Therefore, it is hard to fit a discontinuous PSD with a continuous analytical function. Nonetheless, the performance of the gamma fitted PSDs of graupel, with 14% of data points having correlation coefficients greater than 0.9, is better than that of the exponential fitted PSDs.

The comparison of Figure 1 (exponential fit) and Figure 2 (gamma fit) shows that the PSDs of the gamma function fits can represent the observations better in all three ice-phase hydrometeor categories than those of the exponential function fits.

4. The Mutual Dependence Among Three Parameters in Gamma Functions

Figures 3a–3c show the mutual dependence among intercept (N_0), slope (λ), and shape (μ) the parameters through the scatter plots of λ versus $\log_{10}N_0$ (Figure 3a), λ versus μ (Figure 3b), and μ versus $\log_{10}N_0$ (Figure 3c) for cloud ice PSDs. The fitted curves for the data points with correlation coefficient greater than 0.9 are denoted by the blue lines and the corresponding equation is shown on top of each scatter plot. Figure 3a shows that the relationship between λ and $\log_{10}N_0$ is close to linear, yet a linear relationship will either overestimate N_0 for large λ or underestimate N_0 for small λ. A combination of linear form and exponential form,

$$\log_{10}N_0 = 2.2985 + 0.10800\lambda - 3.1725e^{-0.080000\lambda} \tag{3}$$

is obtained through nonlinear least squares fitting. As it can be seen in Figure 3a, the fitted curve takes on the shape of an exponential function when the slope is smaller than 30 and takes on the shape of a linear

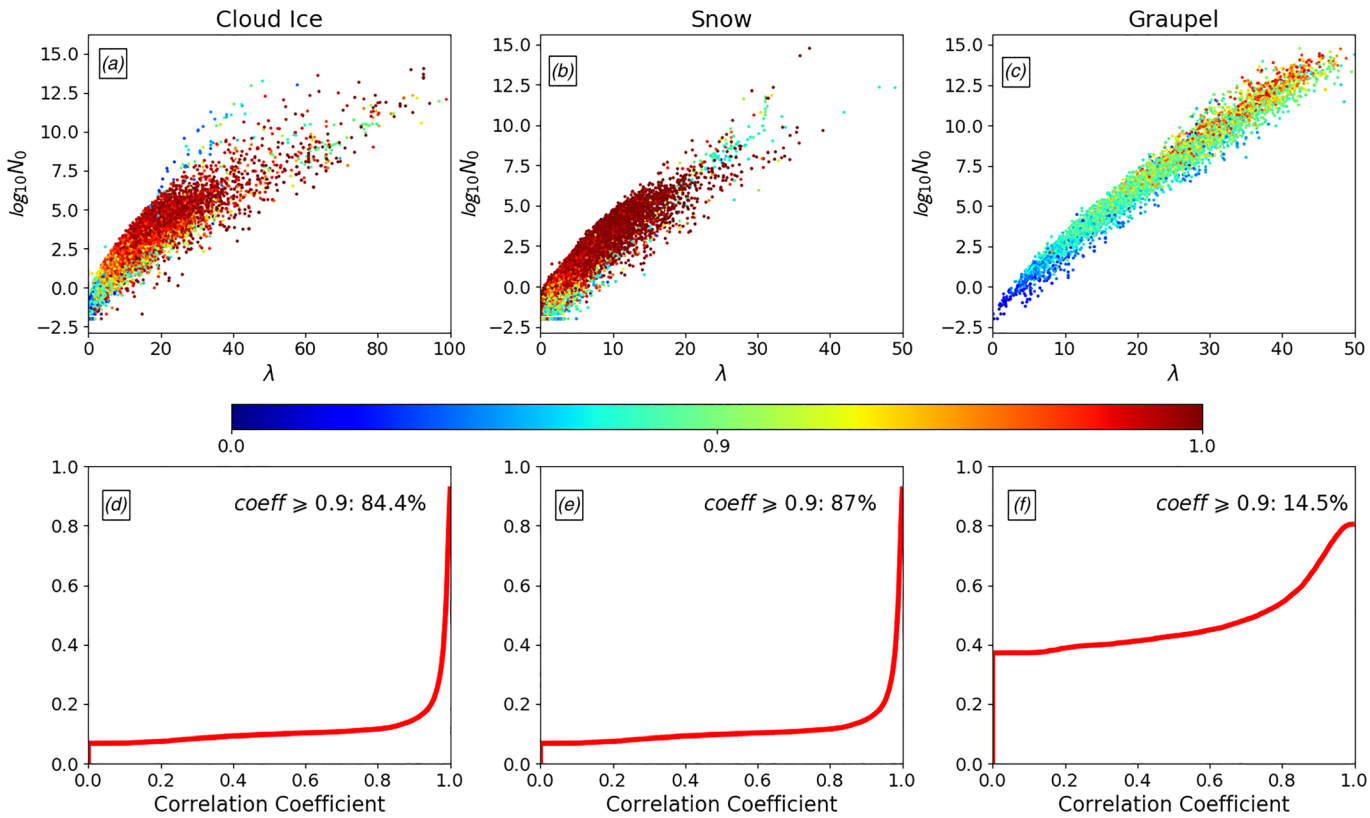

Figure 2. Same as in Figure 1, but for gamma distributions.

function for a slope greater than 30. This analytical form represents the data points reasonably well throughout the whole range of slope parameters. The scatter plot of λ versus μ for cloud ice (Figure 3b) shows that there are two main clusters, red cluster (high correlation coefficient) with an almost linear relationship and blue cluster (low correlation coefficient) with an exponential relationship. There are some data points with intermediate correlation coefficient between these two clusters. The analytic function of the fitted curve to the red cluster has a form similar to the one in Figure 3a and is given by

$$\mu = 1.1100 + 0.080000\lambda - 2.3500e^{-0.080000\lambda} \tag{4}$$

The scatter plot of μ and $\log_{10}N_0$ (Figure 3c) shows that μ and $\log_{10}N_0$ for the data points with high correlation coefficient are linearly related by

$$\log_{10}N_0 = 1.3500\mu + 0.80000 \tag{5}$$

Equation 5 can also be derived from Equations 3 and 4. The mutual dependence of $\mu - \lambda - N_0$ constrained by Equations 3–5 points out that none of the three parameters can be constant, and one has to be prescribed as a function of other prognostic or diagnostic variable(s) in the model.

Figures 3d–3f are the same scatter plots as in Figures 3a–3c except for snow PSDs. Since the patterns seen in Figure 3e–3g are very similar to those in Figures 3a–3c, only the three equations that represent the three analytic curves are given below in Equations 6–8.

$$\log_{10}N_0 = 2.0000 + 0.25000\lambda - 3.1725e^{-0.080000\lambda} \tag{6}$$

$$\mu = 2.4400 + 0.27750\lambda - 3.5215e^{-0.080000\lambda} \tag{7}$$

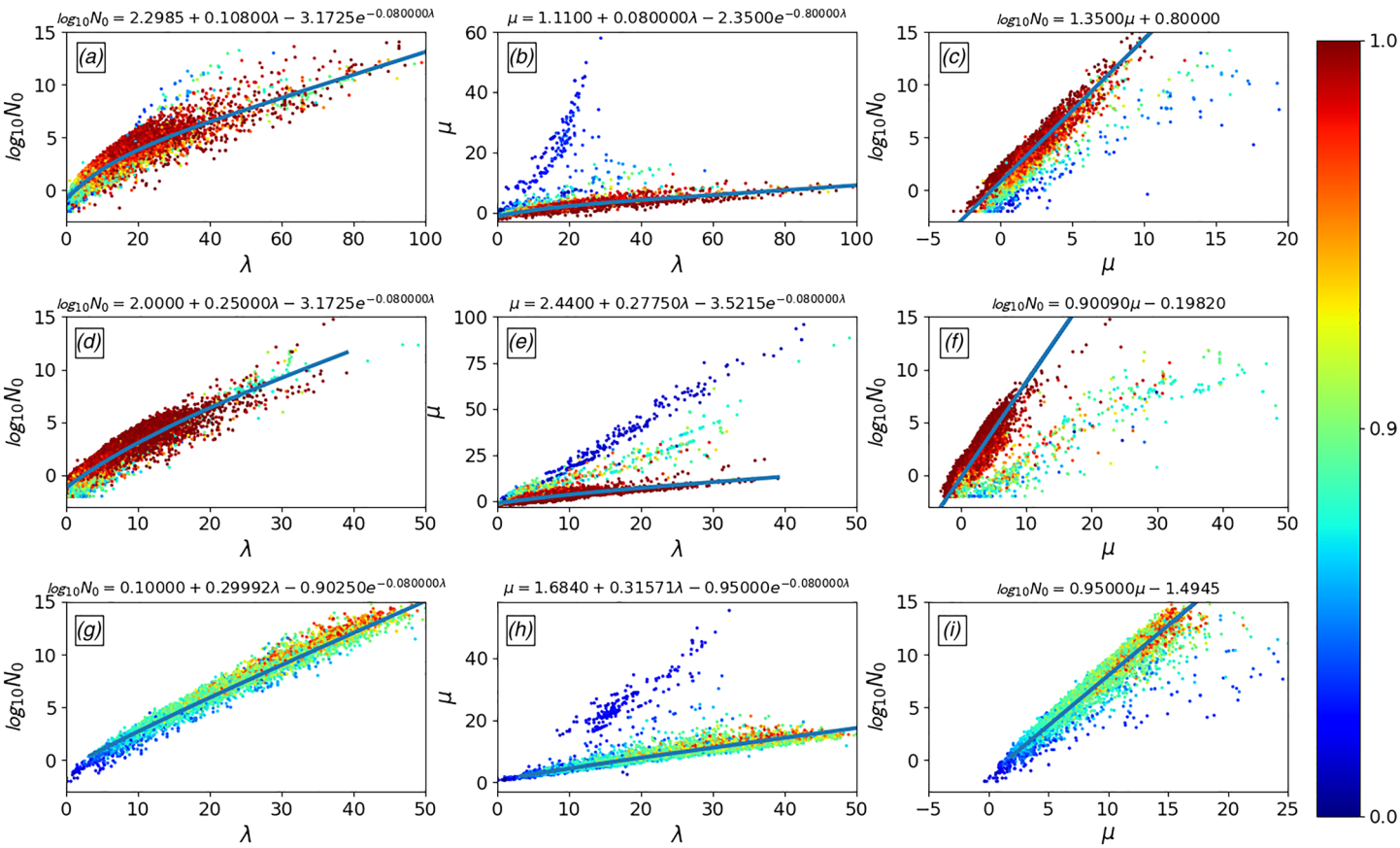

Figure 3. Scatter plots of λ versus $\log(N_0)$ (a), scatter plots of λ versus μ (b), and scatter plots of μ versus $\log(N_0)$ (c) for cloud ice PSDs. Panels (d)–(f) are the same as panels (a)–(c) but for snow PSDs. Panels (g)–(i) are the same as panels (a)–(c) but for graupel PSD. The blue lines denote the fitted curve using data points with correlation coefficient ≥0.9 for cloud ice PSDs and snow PSDs, and with correlation coefficient ≥0.6 for graupel PSDs. The values of correlation coefficients are denoted by the color of data points.

$$\log_{10}N_0 = 0.90090\mu - 0.19820 \tag{8}$$

Figures 3g–3i are the same scatter plots as in Figures 3a–3c except that they are for graupel PSDs, and the fitted curves are for data points with correlation coefficient greater than 0.6 due to low overall correlation coefficient value in graupel. The three equations that represent the three analytic curves are given below in Equations 9–11.

$$\log_{10}N_0 = 0.10000 + 0.29992\lambda - 0.90250e^{-0.080000\lambda} \tag{9}$$

$$\mu = 1.6840 + 0.31571\lambda - 0.95000e^{-0.080000\lambda} \tag{10}$$

$$\log_{10}N_0 = 0.95000\mu - 1.4945 \tag{11}$$

5. The Correlation Between Gamma Function Parameters and Other Variables

As shown in Figure 3, all three parameters in gamma functions are closely correlated to each other. This mutual dependence greatly reduces the dimensional freedom of implementing the gamma fitted PSDs for all ice categories in microphysics schemes.

To determine the gamma fitted PSDs in microphysics schemes, one parameter can be either prescribed or parameterized by other model prognostic variables. In order to establish the relationship between parameters in gamma fitted PSDs and other observed environmental variables, three heatmaps (a heatmap is a two-dimensional graphical representation of data where the individual values that are contained in a

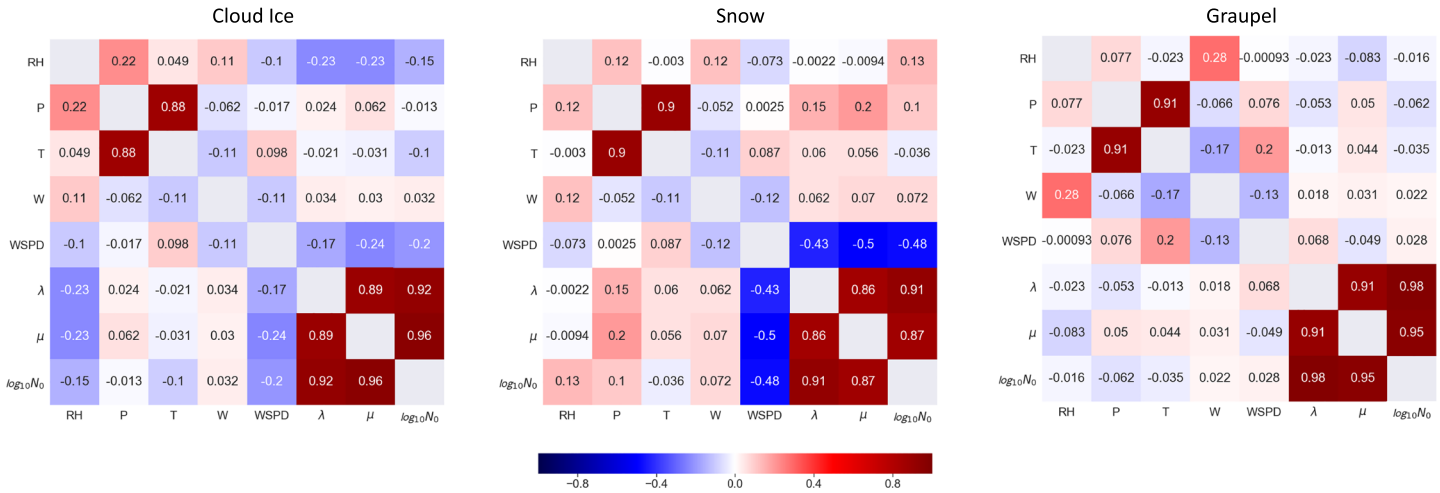

Figure 4. Heatmap of correlation coefficients for (a) cloud ice PSDs, (b) snow PSDs, and (c) graupel PSDs.

matrix are represented as colors, https://pythonbasics.org/seaborn-heatmap/) of correlation coefficients are plotted in Figure 4. The coefficients represent the correlation among all three parameters in the gamma functions of the fitted PSDs, temperature (*T*), relative humidity (*RH*), pressure (*P*), vertical motion (*W*), and wind speed (*WSPD*) for cloud ice, snow, and graupel. The overall patterns of the correlation coefficient matrix for all variables (slope, intercept, dispersion, *T*, *RH*, *P*, *W*, and *WSPD*) are similar in the PSDs for all three ice hydrometeor categories. For example, the high correlation coefficient is only found between *P* and *T* and among all three parameters for the gamma function. However, there are a few less obvious characteristics revealed by the heatmap. The correlation coefficients between temperature and any parameter in the gamma function are very small for all ice PSDs. This seems to be in contradiction to early studies that assumed that the ice PSDs were closely related to temperature (Field et al., 2005; Houze et al., 1979). The correlation coefficient between wind speeds and any parameter in the gamma fitted PSDs, especially for snow, are higher than any thermodynamic and dynamic variable included here. The temperature dependency of PSDs represents the size effect of aggregation, as pointed out by Houze et al. (1979), that the ice particles grow as they drift downward. Heymsfield et al. (2002) also showed that the particle size increased from cloud top to cloud bottom due to the aggregation process by examining the vertical profile of ice particles in the stratiform clouds. The main difference between the observations presented in this study and in previous publications (e.g., Field et al., 2005; Heymsfield et al., 2002; Houze et al., 1979) is that the wind speeds are much higher because the observations were collected in the TC environment. The high winds can disrupt the aggregation process or break up the ice particles that grow from aggregation process.

Heymsfield et al. (2006) showed large aggregates, some larger than 7 mm, in the observations collected between 8.5 and 11 km in a Category 2 Hurricane Humberto (2001). Yet our microphysics observations, which were collected between 5 and 6.5 km, show that the snow particle size rarely exceeds 4 mm. If the ice particle size grows downward, then ice particles larger than 7 mm should be observed between 5 and 6.5 km altitude. One possible explanation for the lack of the temperature dependency of ice PSDs is that ice particles growing through an aggregation process is susceptible to breakup in a high wind environment, which is also implied by the relatively high correlation coefficient between wind speeds and the parameters in gamma fitted PSDs. The wind speeds of TCs decrease with height and the decreasing rate is especially high for shallow or tilted storms. As described in Heymsfield et al. (2006), Hurricane Humberto (2001) was tilted due to shear. The comparison of our microphysics observations collected at 5–6.5 km with the those collected at 8.5–11 km in Heymsfield et al. (2006) implies that the predominant view of ice particle size increasing from cloud top to cloud bottom and associated temperature dependency is not applicable in the TC environment.

Model-simulated radar reflectivity also provided some evidence to support our argument. McFarquhar et al. (2012, 2006) and Rogers et al. (2007) have shown that simulated reflectivity in model simulations is generally higher than observed. Since radar reflectivity is heavily weighted toward the largest hydrometeors due

to the Rayleigh scattering dependence on the sixth power of the particle diameter at centimeter wavelengths (Brown et al., 2016), the larger simulated reflectivity in the model evaluation study suggest that the simulated particles are larger than the observed particles. All the current microphysics schemes in numerical models have not taken into account of the effect of high winds in breaking up the aggregated ice particles, and therefore the TC simulations using these microphysics schemes tend to produce ice particles that are biased toward large size and correspondingly strong radar reflectivity.

6. Summary and Discussion

The comparison of exponential and gamma fits for the microphysics observations collected during eight TC flights demonstrates that gamma fits of the PSDs are better than exponential fits in representing observed ice PSDs. For cloud ice (snow) PSDs, 43% (55%) of exponential PSDs have correlation coefficients greater than 0.9 while 84% (87%) of correlation coefficients of gamma PSDs are greater than 0.9. For graupel PSD, neither exponential fits nor gamma fits can represent the observed PSD well due to the fact that often the observed graupel PSDs are not continuous. Despite the poor performance of both functions for graupel PSDs, gamma fits (15%) still perform better than exponential fits (0%). Another advantage of gamma fits over exponential fits is that all three parameters are closely tied together. Given one parameter, the other two can be rendered based on the analytical functions presented in this study. The mutual dependence among these three parameters simplifies the application of the gamma fitted PSDs to microphysics parameterization schemes.

The heatmap of correlation coefficients among all three parameters in the gamma functions and other dynamic and thermodynamic variables shows that there is no obvious relationship between any parameter and temperature, a variable that is shown to play a paramount role in controlling ice PSDs in previous literatures (Field et al., 2005; Houze et al., 1979). Instead, our results show that wind speeds may play an important role in controlling ice PSDs, especially for snow. The comparison of our results with the previous literature that examined ice PSDs in low-wind environment, such as winter storms (Field et al., 2005) and frontal clouds (Houze et al., 1979), suggests that high wind tends to disrupt the aggregation process and therefore invalidate the previous conclusion of top-down growth of ice particles and the associated temperature dependence of ice PSDs.

Our results suggest gamma fitted PSDs should be used for the ice PSDs in microphysics parameterization schemes, and horizontal wind speeds should be taken into account in the ice PSDs in the high wind environment. These changes in microphysics schemes are expected to change the heating profile through radiative process due to albedo effect associated with breakup of ice particles and therefore smaller drops. They are also anticipated to affect the terminal velocity of ice particles and rain drops.

In the future work, an artificial neural network will be used to uncover the complex relationship between parameters in gamma functions for ice PSDs and environmental variables. Operational hurricane forecast models will be used to evaluate the performance of revised microphysics schemes.

Data Availability Statement

The authors express thanks to NOAA/AOML for hosting the data (ftp.aoml.noaa.gov/pub/hrd/rblack/GRL2).

Acknowledgments
This research had been supported by the NASA Grant NNX17AI60G and EPIC, OAR-Weather Program Office GAP funds. We want to acknowledge our colleagues: John Gamache and Jun Zhang, for their insightful comments to improve this manuscript during our internal review.

References

Black, R., Bluestein, H. B., & Black, M. L. (1994). Unusually strong vertical motions in a Caribbean hurricane. *Monthly Weather Review*, *122*(12), 2722–2739. https://doi.org/10.1175/1520-0493(1994)122<2722:USVMIA>2.0.CO;2

Black, R., & Hallett, J. (1986). Observations of the distributions of ice in hurricanes. *Journal of the Atmospheric Sciences*, *43*(8), 802–822. https://doi.org/10.1175/1520-0469(1986)043<0802:OOTDOI>2.0.CO;2

Black, R., & Hallett, J. (1999). Electrification of the hurricane. *Journal of the Atmospheric Sciences*, *56*(12), 2004–2028. https://doi.org/10.1175/1520-0469(1999)056<2004:EOTH>2.0.CO;2

Black, R. A. (1990). Radar reflectivity–ice water content relationships for use above the melting layer in hurricanes. *Journal of Applied Meteorology*, *29*(9), 955–961. https://doi.org/10.1175/1520-0450(1990)029<0955:RRIWCR>2.0.CO;2

Brown, B. R., Bell, M. M., & Frambach, A. J. (2016). Validation of simulated hurricane drop size distributions using polarimetric radar. *Geophysical Research Letters*, *43*(2), 910–917. https://doi.org/10.1002/2015GL067278

Field, P. R., Hogan, R. J., Brown, P. R. A., Illingworth, A. J., Choularton, T. W., & Cotton, R. J. (2005). Parameterization of ice particle size distributions for mid-latitude stratiform cloud. *Quarterly Journal of the Royal Meteorological Society*, *131*(609), 1997–2017. https://doi.org/10.1256/qj.04.134

Hansen, J. E., & Travis, L. D. (1974). Light scattering in planetary atmospheres. *Space Science Reviews*, *16*, 527–610.

Heymsfield, A. J., Bansemer, A., Durden, S. L., Herman, R. L., & Bui, T. P. (2006). Ice microphysics observations in Hurricane Humberto: Comparison with non-hurricane-generated ice cloud layers. *Journal of the Atmospheric Sciences*, *63*(1), 288–308. https://doi.org/10.1175/JAS3603.1

Heymsfield, A. J., Bansemer, A., Field, P. R., Durden, S. L., Stith, J. L., Dye, J. E., et al. (2002). Observations and parameterizations of particle size distributions in deep tropical cirrus and stratiform precipitating clouds: Results from in situ observations in TRMM field campaigns. *Journal of the Atmospheric Sciences*, *59*(24), 3457–3491. https://doi.org/10.1175/1520-0469(2002)059<3457:OAPOPS>2.0.CO;2

Hong, S.-Y., & Lim, J. J. (2006). The WRF single-moment 6-class microphysics scheme (WSM6). *Journal of Korean Meteorological Society*, *42*(2), 129–151.

Houze, R. A. Jr., Hobbs, P. V., Herzegh, P. H., & Parsons, D. B. (1979). Size distributions of precipitation particles in frontal clouds. *Journal of the Atmospheric Sciences*, *36*(1), 156–162. https://doi.org/10.1175/1520-0469(1979)036<0156:SDOPPI>2.0.CO;2

Houze, R. A. Jr., Marks, F. D. Jr., & Black, R. A. (1992). Dual-aircraft investigation of the inner core of hurricane Norbert. Part II: Mesoscale distribution of ice particles. *Journal of the Atmospheric Sciences*, *49*(11), 943–963. https://doi.org/10.1175/1520-0469(1992)049<0943:DAIOTI>2.0.CO;2

Lin, Y.-L., Farley, R. D., & Orville, H. D. (1983). Bulk parameterization of the snow field in a cloud model. *Journal of Climate and Applied Meteorology*, *22*(6), 1065–1092. https://doi.org/10.1175/1520-0450(1983)022<1065:BPOTSF>2.0.CO;2

Lord, S. J., & Lord, J. M. (1988). Vertical velocity structures in an axisymmetric, nonhydrostatic tropical cyclone model. *Journal of Atmospheric Sciences*, *45*(9), 1453–1461. https://doi.org/10.1175/1520-0469(1988)045<1453:VVSIAA>2.0.CO;2

Lord, S. J., Willoughby, H. E., & Piotrowicz, J. M. (1984). Role of parameterized ice-phase microphysics in an axisymmetric, nonhydrostatic tropical cyclone model. *Journal of Atmospheric Sciences*, *41*(19), 2836–2848. https://doi.org/10.1175/1520-0469(1984)041<2836:ROAPIP>2.0.CO;2

McFarquhar, G. M., & Black, R. A. (2004). Hurricane observations of particle size and phase and their implications for mesoscale modeling of microphysical processes. *Journal of the Atmospheric Sciences*, *61*(4), 422–439.

McFarquhar, G. M., Jewett, B. F., Gilmore, M. S., Nesbitt, S. W., & Hsieh, T.-L. (2012). Vertical velocity and microphysical distributions related to rapid intensification in a simulation of Hurricane Dennis (2005). *Journal of the Atmospheric Sciences*, *69*(12), 3515–3534.

McFarquhar, G. M., Hsieh, T.-L., Freer, M., Mascio, J., & Jewett, B. F. (2015). The characterization of ice hydrometeor gamma size distributions as volumes in N_0-λ-μ phase space: Implications for microphysical process modeling. *Journal of the Atmospheric Sciences*, *72*(2), 892–909.

Marshall, J. S., & Palmer, W. H. (1948). The distribution of raindrops with size. *Journal of Meteorology*, *5*(4), 165–166. https://doi.org/10.1175/1520-0469(1948)005<0165:TDORWS>2.0.CO;2

McFarquhar, G. M., Zhang, H., Heymsfield, G., Halverson, J. B., Hood, R., Dudhia, J., & Marks, F. (2006). Factors affecting the evolution of hurricane Erin (2001) and the distributions of hydrometeors: Role of microphysical processes. *Journal of the Atmospheric Sciences*, *63*(1), 127–150. https://doi.org/10.1175/JAS3590.1

Rogers, R. F., Black, M. L., Chen, S. S., & Black, R. A. (2007). An evaluation of microphysics fields from mesoscale model simulations of tropical cyclones. Part I: Comparisons with observations. *Journal of the Atmospheric Sciences*, *64*(6), 1811–1834.

Sekhon, R. S., & Srivastava, R. C. (1970). Snow size spectra and radar reflectivity. *Journal of Atmospheric Sciences*, *27*(2), 299–307. https://doi.org/10.1175/1520-0469(1970)027<0299:SSSARR>2.0.CO;2

Thompson, G., Field, P. R., Rasmussen, R. M., & Hall, W. D. (2008). Explicit forecasts of winter precipitation using an improved bulk microphysics scheme. Part II: Implementation of a new snow parameterization. *Monthly Weather Review*, *136*(12), 5095–5115. https://doi.org/10.1175/2008MWR2387.1

Ulbrich, C. W. (1983). Natural variations in the analytical form of the raindrop size distribution. *Journal of Climate and Applied Meteorology*, *22*(10), 1764–1775. https://doi.org/10.1175/1520-0450(1983)022<1764:NVITAF>2.0.CO;2

Willoughby, H. E., Jin, H.-L., Lord, S. J., & Piotrowicz, J. M. (1984). Hurricane structure and evolution as simulated by an axisymmetric, nonhydrostatic numerical model. *Journal of the Atmospheric Sciences*, *41*(7), 1169–1186. https://doi.org/10.1175/1520-0469(1984)041<1169:HSAEAS>2.0.CO;2